Facile fabrication of YSZ/GDC multi-layers by using a split target in pulsed laser deposition and their structural and electrical properties

Jung Hoon Park · Wan-Shick Hong · Jong-Ho Lee · Kyung Joong Yoon · Hyoungchul Kim · Jongsup Hong · Hue-Sup Song · Ji-Won Son

Abstract Various configurations of the multi-layer of yttria-stabilized zirconia (YSZ) and gadolinia-doped ceria (GDC) are successfully fabricated through a novel method by means of pulsed laser deposition (PLD) utilizing a split target. By controlling the deposition conditions like the laser frequency and target configuration, YSZ/GDC multi-layers of different periodicities and YSZ/GDC thickness ratios can be easily and simply realized. The multi-layer fabricated by the proposed method exhibits nearly identical physical and electrical properties to those of the multi-layer films by the conventional layer-by-layer deposition method. The present study provides a facile and effective fabrication method for the design and application of multi-layered structure.

Keywords Multi-layer thin films · Pulsed laser deposition · Split target · YSZ · GDC

1 Introduction

Multi-layer thin films consisting of hetero-materials have been investigated in many areas because of the extraordinary properties induced by the interfacial effect. For example, the

J. H. Park · J.-H. Lee · K. J. Yoon · H. Kim · J. Hong ·
J.-W. Son (✉)
High-temperature Energy Materials Research Center, Korea Institute of Science and Technology, Seoul 136-791, South Korea
e-mail: jwson@kist.re.kr

J. H. Park · W.-S. Hong
Department of Nano Science and Technology, University of Seoul, Seoul 130-743, South Korea

H.-S. Song
Division of Advanced Materials Engineering, Kongju National University, Kongju 314-701, South Korea

mechanical property of multi-layered structural materials is greatly improved because the dislocations cannot propagate in the alternating nano-layers [1–3]. It has been reported that an increase of the interface density in a two-phase multi-layered structure drastically enhances the ion conductance of the material [4–6]. For this reason, multi-layered oxide thin films are often at the center of interests for solid state electrochemical devices, e.g. sensors, capacitors and solid oxide fuel cells (SOFCs) [7, 8]. Especially in the field of the SOFC, the multi-layered electrolyte materials draw intensive attention. This is because high ionic conductivity at low temperatures is essential to improve the performance and lifetime of the SOFC [9, 10], thus the search for new electrolyte materials has been researched extensively [11–14]. Nevertheless, since novel electrolyte materials have drawbacks like chemical and physical instabilities, existing electrolytes that can be used to improve the performance by optimizing their microstructure have been more actively investigated [15–19]. As a part of these research efforts, the multi-layered electrolyte has been much studied and has exhibited great potentials [7, 20–23].

The multi-layered structure can be deposited by means of a variety of existing methods. In principle, the targets or sources of the different materials are switched during the deposition. Although this appears simple, the actual fabrication process can be quite cumbersome. The process requires a long time for the deposition and precise control of the process condition depending on materials. Otherwise, the various experimental errors, such as the loss of periodicity, may occur, which may incur undesirable outcomes like loss of the targeted properties. In order to facilitate the fabrication of the multi-layered structure, we propose a new method of pulsed laser deposition (PLD) utilizing a split target. For different but similar materials that the films of those can be deposited at the similar environment, this can be a substantially effective, simple, and

precise method to fabricate multi-layered structures. In the thin film deposition using the PLD method, only part of the target is irradiated by a focused laser beam and the target is rotated for uniform erosion of the target (Fig. 1(a)). If the target surface is split physically by more than two materials as shown in Fig. 1(b), the source material used for deposition can be altered by simple rotation when the beam position is fixed. The configuration of the multi-layer such as the thickness of each layers, number of consisting materials, etc., can be controlled by changing the target rotation speed, the laser frequency, and the portion of each material in the target.

To prove the concept of the method, we fabricate multi-layered structures consisting of yttria-stabilized zirconia (YSZ) and gadolinia-doped ceria (GDC) in this study. YSZ is the most common electrolyte material of the SOFC because of its high chemical stability and negligible electron conductivity in a wide range of oxygen partial pressure. Nevertheless, the ionic conductivity of YSZ is too low to be used at the low temperature. GDC is an alternative electrolyte material that has a higher ionic conductivity than that of YSZ, however, relatively high electronic conductivity of GDC is a significant issue, especially when GDC is exposed to a reducing atmosphere (anode side). Through the realization of the multi-layered structure of YSZ and GDC, we expect the improvement of the performance of the electrolyte by suppressing the weakness of each material and by inducing the enhanced ionic conductivity owing to the hetero-interface effect.

In the present study, various multi-layered structures of YSZ/GDC are deposited by using split targets of YSZ and GDC and by changing the frequency of the laser and the target configuration. The analyses of physical properties such as the periodicity and microstructure of the YSZ/GDC multi-layer are performed. The electrical properties of the YSZ/GDC multi-layers are also investigated by impedance analyses. Differences between the multi-layers by the proposed method and by the general, one layer by one layer deposition method are compared in term of the physical and electrical properties.

2 Experimental

For PLD, a KrF excimer laser (λ=248 nm, COMPEX Pro 201 F, Coherent) was used as a laser source. The target-to-substrate distance was 5 cm, and the laser energy density was 2.5 J•cm^{-2} at the target surface. The substrate temperature (T_s) was maintained at 700 °C, and the ambient oxygen pressure (P_{amb}) was maintained at 6.67 Pa during the deposition process. Multi-layered thin films were deposited on (0001)-oriented polished single crystal Al_2O_3 (sapphire). YSZ and GDC targets were prepared by sintering a compact pellet of each powder. Commercial YSZ (8 mol% Y_2O_3-stabilized ZrO_2, TZ-8Y, Tosoh Corp., Japan) and GDC ($Gd_{0.1}Ce_{0.9}O_{1.95-\delta}$, Rhodia, France) powders were uniaxially pressed (50 MPa) and sintered (5 h at 1500 °C). We prepared a half-half target and a quarter target as shown in Fig. 2(a). The target rotation speed was fixed as 2 rpm and the laser frequency was varied between 10 Hz and 2 Hz for the deposition rate adjustment as shown Fig. 2(a). The multi-layered thin film specimens will be denoted as H-10, H-2, and Q-10, respectively. H stands for the
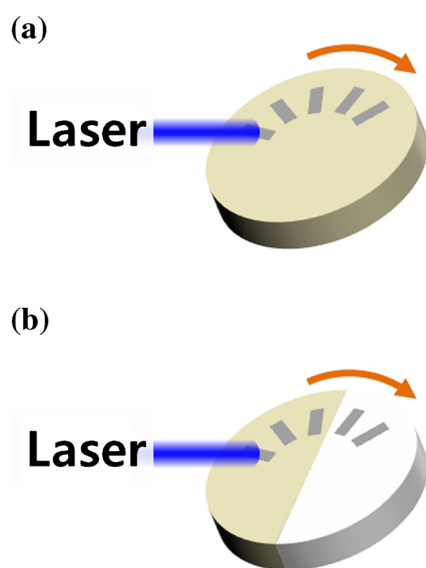

Fig. 1 Schematics showing the ablation of the target in (a) a general PLD and (b) the proposed PLD method
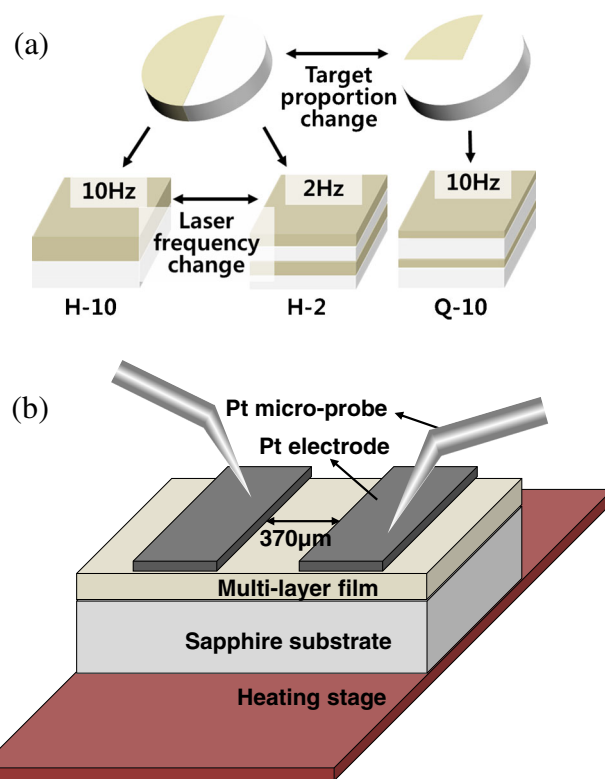

Fig. 2 (a) Target configuration and laser frequencies used in the present study. (b) A schematic showing the in-plane conductivity measurement

half-half target and Q stands for the 1/4–3/4 target, and the number stands for the laser frequency.

Transmission electron microscopy (TEM, TitanTM, FEI) was used to characterize microstructural properties. The thickness and composition of the individual layers in the multi-layer were confirmed with images and energy dispersive spectroscopy (EDS) of TEM, respectively. In addition, the interface between layers was analyzed by high resolution TEM imaging. For electrical characterization, an in-plane conductivity measurement was performed [24]. Parallel strip-shaped Pt electrodes (3.1 mm by 0.64 mm) were deposited by DC magnetron sputtering on the surface of the film. The gap between the strips was 370 μm. The electrodes were contacted using Pt probes as shown in Fig. 2(b). Impedance measurements were performed using a Solatron impedance analyzer (SI1260) with an electrochemical interface (SI1287). The samples were heated by a heating stage and were analyzed in ambient air. The temperature was varied from 600 to 350 °C at a 50 °C interval, and the impedance spectra (IS) were obtained at each temperature in a frequency range from 1 MHz to 0.1 Hz.

3 Results and discussion

Figure 3 shows the TEM image of each sample. Figure 3(a), (b), and (c) are high-angle annular dark field (HAADF) images of aforementioned H-10, H-2, and Q-10, respectively. In the image, the bright part is the GDC region, the dark part is the YSZ region. As expected, multi-layered structures were successfully fabricated with various configurations. When using the same half-half target and changing the laser frequency (H-10, H-2, shown in Fig. 3 (a) and (b)), the thickness ratio of YSZ to GDC was same but the period of multi-layer of both specimens was different. For an increased laser frequency, the number of laser pulses in the certain region of target, YSZ or GDC, is increased. Therefore, the thickness of each layer is increased. From these results, it is confirmed that the period of the multi-layer can be controlled by this parameter. It is also notable that for H-10 and H-2, the thickness ratio of YSZ to GDC is not 1:1. This is because that the deposition rate of GDC is approximately 2~3 times higher than that of YSZ. To make the YSZ/GDC thickness ratio near to unity, the quarter target was used and it is shown that the thickness of each layer is almost equivalent for Q-10 shown in Fig. 3(c)). Therefore, from this result, it is proven that the configuration of one period of the multi-layer can be controlled easily by modification of the portion of each material in the target.

In Fig. 3(d), the microstructure of the multi-layer deposited by conventional layer-by-layer fabrication, which is prepared for the comparison, is shown. This sample will be denoted as CM (conventional method). It was deposited at the process conditions to produce the identical period and the YSZ/GDC

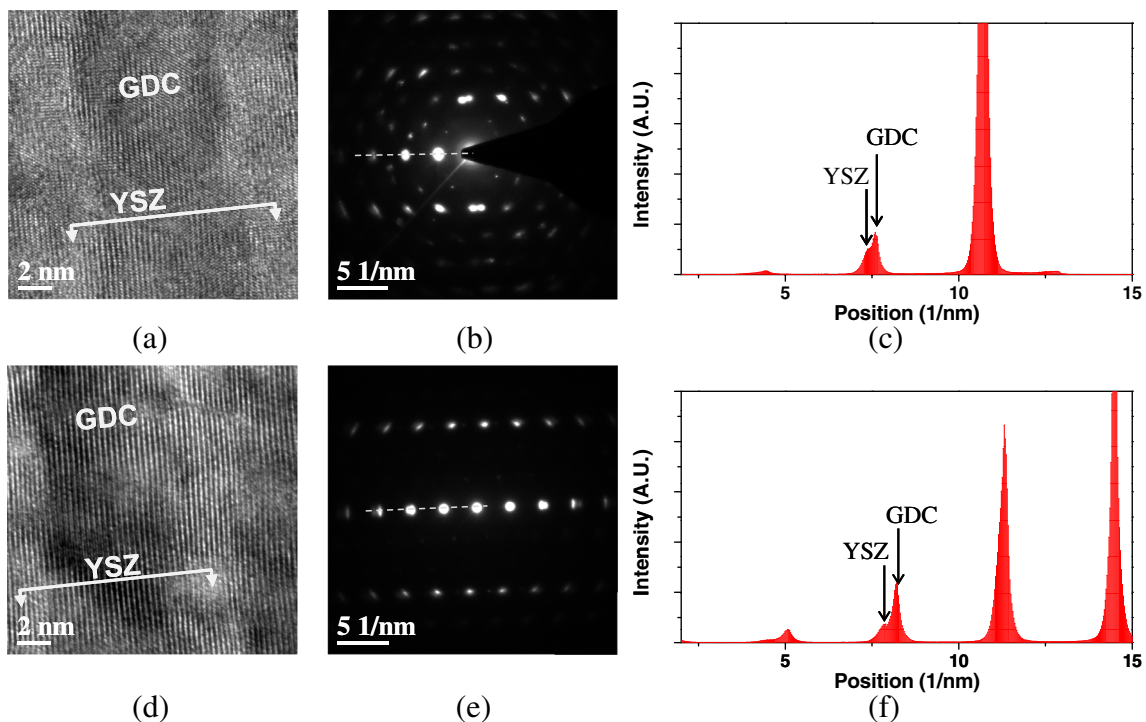Fig. 3 HADDF images of the multi-layers of (a) H-10; (b) H-2; (c) Q-10; and (d) CM
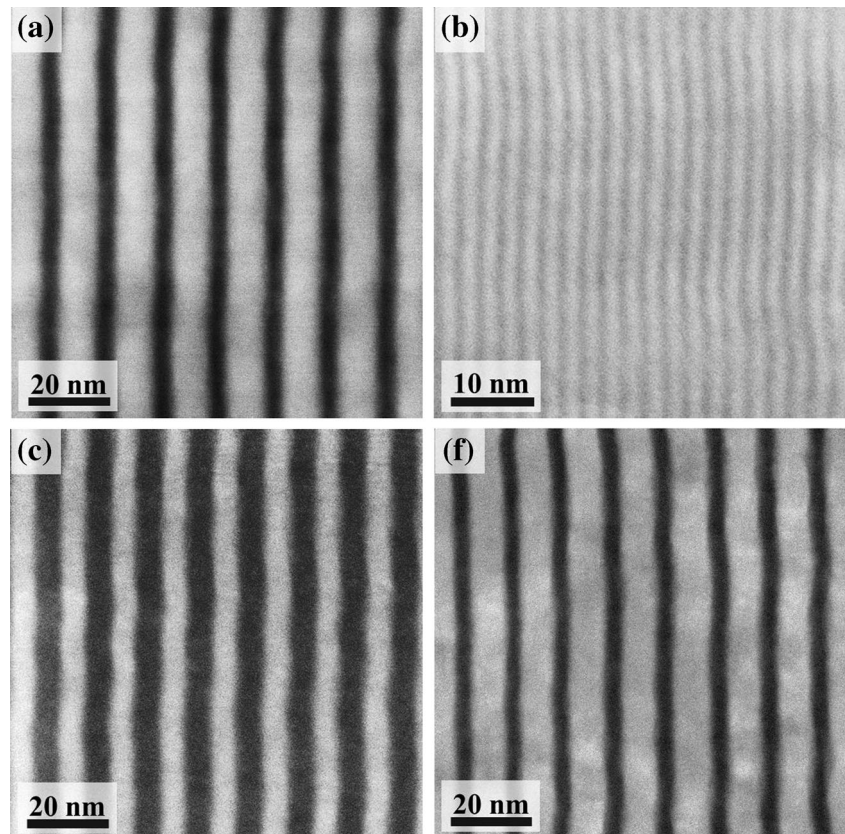
Fig. 4 (**a**), (**d**) HR-TEM bright field images; (**b**), (**e**) electron diffraction patterns; and (**c**), (**f**) line profiles of the *dotted lines* of (**b**) and (**e**) of H-10 (upper) and CM (lower), respectively

ratio to H-10, by controlling the number of laser pulses on the alternating targets. In the HAADF image, it can be observed that the microstructures of both of sample are almost the same. In order to investigate the microstructural properties H-10 and CM in more detail, HR-TEM was used. Figure 4(a) and (d) are HR-TEM images of H-10 and CM. Since the lattice constants of YSZ(c=5.14 Å) and GDC(c=5.42 Å) are slightly different while the crystal structure of YSZ and GDC is the same (fluorite structure), a hetero-epitaxial relation was expected. The lattice of each layer for both cases is continuous across the interface, which indicates that the epitaxial interface is formed as expected. However, slight difference of crystallinity was observed in electron diffraction patterns from wider areas, as

shown in Fig. 4(b), (e). Although the lattices of the both cases were highly textured, slight disorders such as tilted lattices and low angle boundaries exist in H-10, which are shown as the displaced spots in Fig. 4(b). In contrast, such disordered spots were not found in the diffraction pattern of the CM shown in Fig. 4(e). It is postulated that each layer of CM to be stabilized during the target-switching dwell time. On the other hand, continuous deposition of H-10 may yield rather tilted and disoriented growth.

Figure 4(c) and (f) is the line profile of the electron diffraction of each sample (dotted line in Fig. 4(b) and (e)). From Fig. 4(c) and (f), the spacings of (111) planes of YSZ and GDC are deduced for each specimen. For H-10, the (111)

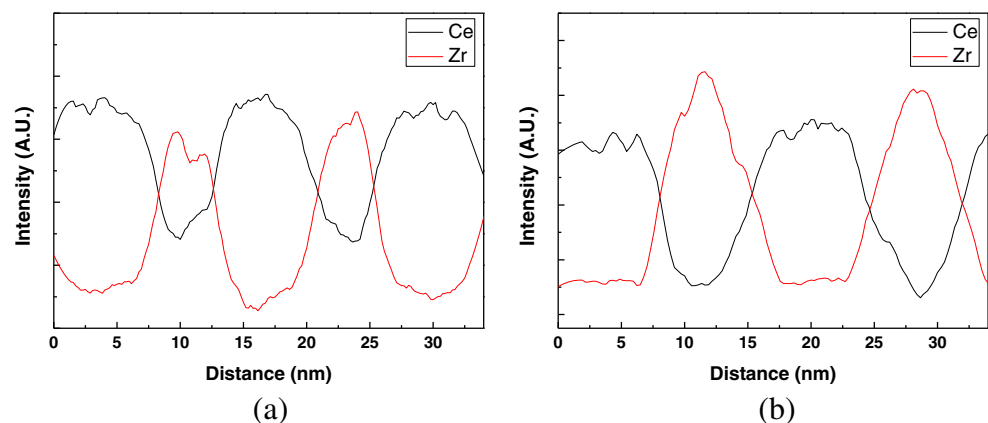**Fig. 5** Ce and Zr elemental distributions in (**a**) H-10 and (**b**) CM
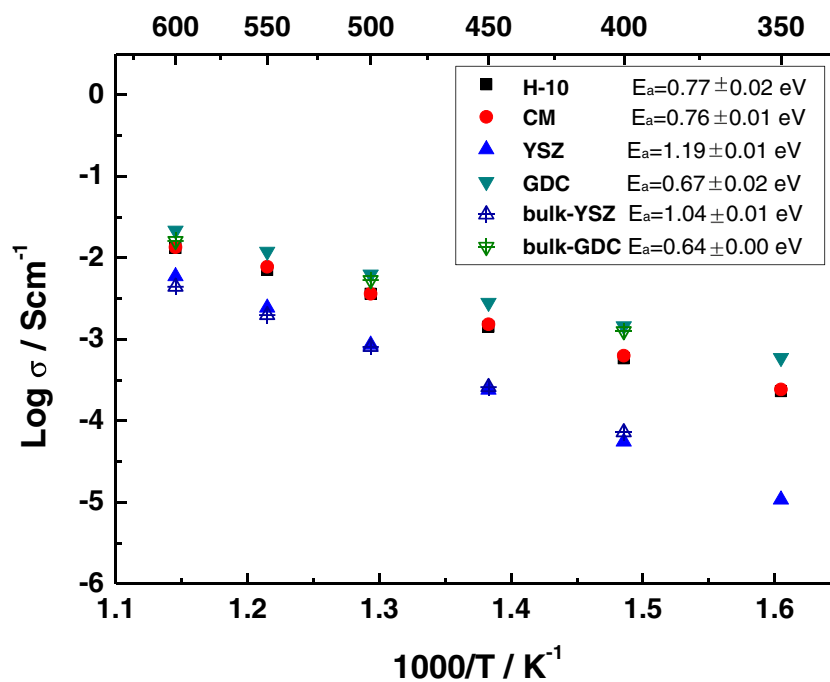
Fig. 6 Electrical conductivity comparison of H-10, CM, YSZ, GDC. The conductivity values of bulk YSZ and GDC are displayed as well

spacing of YSZ is 2.98 Å and that of GDC is 3.19 Å, and for CM, those of YSZ and GDC are 2.98 Å and 3.18 Å, respectively. These spacings are larger than reported values (YSZ=2.971 Å, GDC=3.128 Å). Because both lattices are elongated along the out-of-the plane direction, it appears that both YSZ and GDC are strained by the substrate, not by each other.

Figure 5 shows compositional line profiles obtained from EDS analyses of H-10 and CM. The elemental distribution of Cerium and Zirconium were analyzed, and both cases show distinctive, alternating elemental distribution for each layer. In the case of H-10, however, it appears that the composition mixing occurred more than that in CM, which is thought to be originated from the continuous deposition as well. Nevertheless, although slight differences exist, it can be concluded that near identical multi-layered structure can be fabricated by the proposed method to that by the conventional method, from the microstructural analyses results.

To investigate how the microstructural differences affect the electrical property, the conductivities of H-10 and CM were measured and compared. The thicknesses of both films were approximately 400 nm. Figure 6 shows the Arrhenius plot of the electrical conductivity measured in ambient air at the temperature range of 350~600 °C. The conductivities of H-10 and CM are almost identical, which indicates the multi-layer prepared by the proposed method yields almost identical property to that of conventionally prepared one. Figure 6 also reports the conductivity of an YSZ single-layer film (thickness~1 μm) and a GDC single-layer film (thickness~1 μm) deposited by PLD. It was confirmed that the conductivity of

each single layer film measured in the present study is almost identical to that of the bulk sample. Also, the conductivity of the multi-layer film is almost equal to the calculated conductivity from the conductivity of the single layer multiplied by the volume fraction each material in the multi-layer. An extraordinary ionic conductivity enhancement was not observed in both H-10 and CM. Since CM does not show the conductivity enhancement as well, the multi-layer configuration of this study may not be in the regime where the promoting interfacial effect exists. Although the enhancement was not obtained, the present study demonstrates the proposed method can produce multi-layered structure almost identical to that of the conventional method both in terms of the microstructural and electrical properties quite effectively.

4 Conclusion

Based on the novel proposed method using split targets in PLD, various multi-layered structures of YSZ and GDC are successfully fabricated. The configuration of multi-layers can be easily and simply controlled by changing the laser repetition rate and the target configuration. Except for minor imperfections, the specimen fabricated by the proposed method exhibits almost identical microstructural properties to those of the films by the conventional method. The electrical conductivities are compared and the multi-layers by both methods show almost equal values as well. It is thought that the present study will provide a facile and effective fabrication method for the design and application of multi-layered structure.

References

1. J.S. Koehler, Phys. Rev. B **2**, 547–551 (1970)
2. P.C. Yashar, W.D. Sproul, Vacuum **55**, 179–190 (1999)
3. P. Yashar, S.A. Barnett, J. Rechner, W.D. Sproul, J. Vac. Sci. Technol. A: Vac. Surf. Films. **16**, 2913–2918 (1998)
4. N. Sata, K. Eberman, K. Eberl, J. Maier, Nature **408**, 946–949 (2000)
5. A. Ohtomo, H.Y. Hwang, Nature **427**, 423–426 (2004)
6. X. Guo, J. Maier, Adv. Mater. **21**, 2619–2631 (2009)
7. H. Aydin, C. Korte, M. Rohnke, J. Janek, Phys. Chem. Chem. Phys. **15**, 1944–1955 (2013)
8. A. Peters, C. Korte, D. Hesse, N. Zakharov, J. Janek, Solid State Ionics **178**, 67–76 (2007)
9. E.D. Wachsman, K.T. Lee, Science **334**, 935–939 (2011)
10. B.C.H. Steele, A. Heinzel, Nature **414**, 345–352 (2001)
11. X. Kuang, M.A. Green, H. Niu, P. Zajdel, C. Dickinson, J.B. Claridge, L. Jantsky, M.J. Rosseinsky, Nat. Mater. **7**, 498–504 (2008)
12. E. Kendrick, J. Kendrick, K.S. Knight, M.S. Islam, P.R. Slater, Nat. Mater. **6**, 871–875 (2007)
13. D. Pergolesi, E. Fabbri, A. D'Epifanio, E. Di Bartolomeo, A. Tebano, S. Sanna, S. Licoccia, G. Balestrino, E. Traversa, Nat. Mater. **9**, 846–852 (2010)
14. C. Zuo, S. Zha, M. Liu, M. Hatano, M. Uchiyama, Adv. Mater. **18**, 3318–3320 (2006)
15. J. Jiang, X. Hu, W. Shen, C. Ni, J.L. Hertz, Appl. Phys. Lett. **102**, 143901–143904 (2013)
16. S. Sanna, V. Esposito, D. Pergolesi, A. Orsini, A. Tebano, S. Licoccia, G. Balestrino, E. Traversa, Adv. Funct. Mater. **19**, 1713–1719 (2009)
17. M. Sillassen, P. Eklund, N. Pryds, E. Johnson, U. Helmersson, J. Bøttiger, Adv. Funct. Mater. **20**, 2071–2076 (2010)
18. J.S. Ahn, D. Pergolesi, M.A. Camaratta, H. Yoon, B.W. Lee, K.T. Lee, D.W. Jung, E. Traversa, E.D. Wachsman, Electrochem. Commun. **11**, 1504–1507 (2009)
19. H.-S. Noh, J.-W. Son, H. Lee, H.-S. Song, H.-W. Lee, J.-H. Lee, J. Electrochem. Soc. **156**, B1484–B1490 (2009)
20. J. Garcia-Barriocanal, A. Rivera-Calzada, M. Varela, Z. Sefrioui, E. Iborra, C. Leon, S.J. Pennycook, J. Santamaria, Science **321**, 676–680 (2008)
21. S. Azad, O.A. Marina, C.M. Wang, L. Saraf, V. Shutthanandan, D.E. McCready, A. El-Azab, J.E. Jaffe, M.H. Engelhard, C.H.F. Peden, S. Thevuthasan, Appl. Phys. Lett. **86**, 131906–131903 (2005)
22. B. Li, J. Zhang, T. Kaspar, V. Shutthanandan, R.C. Ewing, J. Lian, Phys. Chem. Chem. Phys. **15**, 1296–1301 (2013)
23. D. Pergolesi, E. Fabbri, S.N. Cook, V. Roddatis, E. Traversa, J.A. Kilner, ACS Nano **6**, 10524–10534 (2012)
24. S. Kim, J.-W. Son, K.-R. Lee, H. Kim, H.-R. Kim, H.-W. Lee, J.-H. Lee, J. Electroceram. **24**, 153–160 (2010)